

## Heavy ion results from the CMS Collaboration

---

**Olga Evdokimov\*** *for the CMS Collaboration*

*University of Illinois at Chicago*

*E-mail: [evdolga@uic.edu](mailto:evdolga@uic.edu)*

The first heavy ion run at the LHC occurred in November of 2010 and was followed by a second run in late 2011 that increased significantly the available event sample achieving integrated luminosity of  $150 \mu\text{b}^{-1}$ . Heavy ion collisions at the LHC are expected to produce a partonic medium which has a higher energy density and a longer life-time than could be created at RHIC. This work gives an overview of what has been learned about the nature of the hot and dense medium created in high energy heavy ion collisions using new data from the CMS experiment. Specifically, azimuthal anisotropy at high transverse momentum, collection of nuclear modification factor measurements for different particle species and identified jets, differential jet properties, and quarkonia measurements are discussed.

*International Winter Meeting on Nuclear Physics,  
21-25 January 2013  
Bormio, Italy*

---

\*Speaker.

## 1. Introduction

High energy heavy ion collisions provide unique environment to study nuclear matter at the extremes of temperature and energy density. They allow for experimental tests of theoretical framework for strong interactions provided by Quantum Chromodynamics (QCD). The first heavy ion collisions delivered by the LHC in 2010 allowed experimental access to the highest energy density medium created in the laboratory. The results obtained from these early PbPb data collected by the CMS experiment [1] at a center-of-mass energy of 2.76 TeV have shown that the matter created in these collisions is indeed strongly interacting, explosive, and exhibits collective behavior [2, 3]. In the following year, CMS continued taking PbPb data at the same energy, recording an event sample corresponding to an integrated luminosity of about  $150 \mu b^{-1}$  (more than 10-fold increase from the first run). This sample extended significantly the kinematic reach for rare probes and processes, particularly in the "hard" sector (high energy or transverse momentum) and heavy flavor studies. In this work an overview of selected recent CMS heavy ion results from 2011 run is presented. Only mid-rapidity measurements are included here, specifically, azimuthal anisotropy at high transverse momentum ( $p_T$ ), collection of nuclear modification factor measurements for different particle species and identified jets, jet shapes and fragmentation functions, and quarkonia measurements. Complete collection of all published and submitted CMS heavy ion papers and preliminary heavy ion results can be found at [4].

## 2. Experimental Setup

Although the CMS detector was not originally conceived specifically for heavy ion physics studies, the versatile system is exceptionally equipped to explore a wide range of related physics topics. CMS is a multi-layer detector, providing nearly  $4\pi$  coverage with a silicon tracking system nested inside high granularity electromagnetic (ECAL) and hadronic (HCAL) calorimeters, in turn enclosed by the muon tracker system. A set of forward detectors (HF, TOTEM, CASTOR, and ZDC) extends acceptance to over 8 units of pseudo-rapidity ( $\eta$ ). These forward detectors allow to test the limiting fragmentation, gluon saturation and color-glass-condensate ideas in new regions of parton momentum fraction  $x$ .

The silicon tracker design allows excellent performance in the high multiplicity environment typical for high energy heavy ion events, and provides acceptance for tracks with momentum above 300 MeV/c with momentum resolutions that is better than 2% for 100 GeV/c tracks. The tracker alone makes study of many physics topics possible; for example, charged particle multiplicity, azimuthal distributions, spectra and correlations of charged particles, that help constrain initial state gluon densities, collective flow and medium viscosity in models. The track pointing resolution of the silicon system also permits statistical identification of displaced vertices, essential for heavy flavor studies. The ECAL granularity ( $0.087 \times 0.087$  at central rapidities) allows direct identification and reconstruction of jets and di-jets. Combination of the ECAL, HCAL and tracker information allows detailed studies of the medium effects on jet properties. Unsurpassed capabilities of muon system allow to resolve quarkonium states and disentangle various productions mechanisms and medium-induced suppression. Last, but not least, the CMS High Level Trigger utilized during the heavy ion data taking extended the energy reach for jets to above 300 GeV, provided access to

ultra-central collisions, and significantly improved the reach for detailed studies of  $J/\psi$ ,  $Z_0$ , and  $\Upsilon$  production as a function of transverse momentum and centrality, which is defined as a fraction of the total geometric cross section, with 0% denoting the most central collisions (zero impact parameter), and 100% - the most peripheral collisions.

### 3. Azimuthal Anisotropy

The strong azimuthal anisotropy observed at RHIC in the angular correlations of final state particles with respect to the event plane is found to be well described by hydrodynamic calculations with little or no viscosity. These measurements have established some of the most important properties of the medium, provided strong evidence for its partonic nature and led to establishing of its “perfect liquid” properties (see, for example, [5] and references therein). It is recognized that the collective expansion of the medium under path-dependent pressure gradients is responsible for the development of the final state azimuthal anisotropies in softer hadrons, while at high  $p_T$  jet quenching, or path-dependent energy loss, produces variations of particle densities with respect to event plane orientation. Within the first year of operations CMS results confirmed the near-perfect liquid behavior in the new energy domain. Here, the extension of these measurements from the run 2011 data is discussed.

To characterize anisotropy in the particle azimuthal distributions with respect to a relevant event plane typically a Fourier expansion of the relative azimuth ( $\Delta\phi$ ) correlation for pairs of charged hadrons is performed. It is expected in theory that the anisotropies of the azimuthal distribution, studied in terms of  $v_n$  coefficients of Fourier expansion, will be sensitive to the early partonic properties of the system. Until recently, experimental measurements were focused on just one harmonic of Fourier expansion,  $v_2$ , often termed “elliptic flow”. Under the simplistic assumption of smooth initial conditions, the higher terms, and all odd terms in general, were expected to be subdominant or extinguished by symmetry. Theoretical developments in recent years led to recognition of importance of the initial state non-uniformity caused by density/geometry fluctuations, which result in the significant anisotropies of higher orders. The evolution of the flow harmonics of all orders with initial eccentricities and energy densities provides experimental constraints on the initial state properties, and the shear viscosity over entropy density ratio ( $\eta/s$ ) during the subsequent system evolution.

CMS has studied in detail the centrality and transverse momentum dependence of the azimuthal anisotropy coefficients  $v_2$ ,  $v_3$ ,  $v_4$ ,  $v_5$  and  $v_6$  in minimum bias PbPb collisions at  $\sqrt{s_{NN}}=2.76$  TeV. Figure 1 shows results of this study [6] for second through fifth harmonics for a mid-central bin, corresponding to 30-35% of total geometric cross-section. Finite values observed for the odd harmonics ( $v_3$ ,  $v_5$ ) illustrate the effects and importance of initial state fluctuations. The

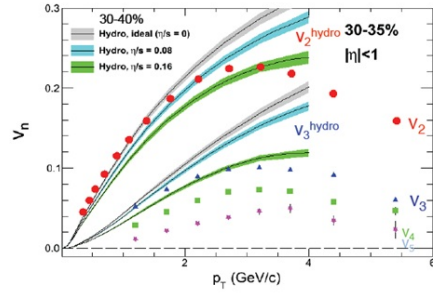


**Figure 1:** Transverse momentum dependence of the Fourier expansion coefficients for mid-central events corresponding to 30-35% of total geometric cross-section. The lines illustrate expectations from hydrodynamic model with different  $\eta/s$  settings from [7].

hierarchy of  $v_n$  magnitudes observed is consistent with theoretical expectations from hydrodynamic evolution of the system. Comparisons with model calculations for the second and third harmonics with various input shear viscosity over entropy density ratios [7] favors  $\eta/s$  values that are non-zero yet close to the expected quantum limit.

At low transverse momentum, the second order harmonic,  $v_2$ , is a dominant anisotropic term of Fourier expansion for most of the impact parameter range of the collisions due to the initial state spacial eccentricity. The magnitudes of  $v_2$  and  $v_3$  become comparable in ultra-central collisions. As noted earlier, the strength of the elliptic flow is found to be approaching the ideal hydrodynamic limit in the low transverse momentum region. It has been found that the elliptic anisotropy persists to much higher momenta, that would be considered reasonable for hydrodynamic treatment of the system. At high  $p_T$  the path-length-dependent partonic energy loss is considered as a primary source for the observed  $v_2$ . Figure 2 shows recent CMS results from run 2011 data for two selected centrality bins. For both selections, 10% most central and 40-50% mid-central events, significant anisotropy persist to transverse momenta of at least 40 GeV/c.

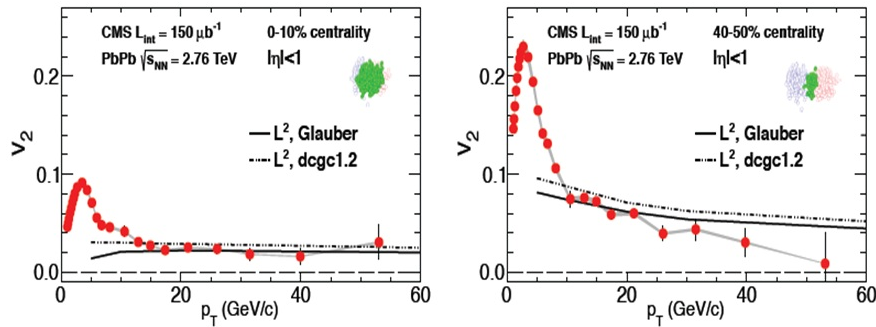


**Figure 2:** Elliptic anisotropy ( $v_2$ ) as function of transverse momentum for 10% most central collisions (a) and events from the 40-50% centrality bin (b). Theoretical calculations from [9] are compared with the data. The model results for radiative energy loss are shown for Glauber (solid line) and Color Glass Condensate (dashed line) initial conditions.

High precision measurements of  $v_2$  vs.  $p_T$ , to large extent enabled by successful implementation of a corresponding High Level Trigger algorithm during 2011 run, allow to constrain significantly the path-length dependence of energy loss in the models, and/or determine the dominant mechanisms for jet quenching. Linear or quadratic dependencies are expected in perturbative QCD for collisional or radiative energy loss scenarios (respectively), while more exotic theories predict stronger (cubic) trends. In Fig. 2 direct comparison with one available perturbative calculation for radiative energy loss mechanism [9] is shown to capture the data trends for both centrality bins quite closely. Additional studies are underway to further quantify the agreement and explore the sensitivity to different types of initial conditions tested.

#### 4. Jet quenching

The effects of the jet energy loss or quenching that lead to the azimuthal anisotropies of particle distributions with respect to event plane at high transverse momenta, as discussed above, could be studied through comparative analysis of inclusive particle distributions in PbPb and pp collisions

at the same energy. To compare the relative particle abundances produced by the two different systems, nuclear modification factors,  $R_{AA}$ , are constructed for each centrality bin of PbPb data by dividing the transverse momentum spectrum measured in this bin by the pp reference spectrum, scaled appropriately by the corresponding nuclear overlap function,  $T_{AA}$  (detailed definitions are provided in citeCMSHRAA). The exact  $T_{AA}$  values are model-dependent, but experimental confirmation of the overlap functions is obtained by constructing nuclear modification factors for the probes that do not interact strongly, and therefore are not expected to suffer energy loss in the colored medium. Figure 3 (a) shows  $R_{AA}$  measurements for isolated photons [10],  $W$ - and  $Z$ -bosons [11, 12] as function of the transverse mass. All three of these measurements are found consistent with unity, confirming the calculated  $T_{AA}$  values give appropriate scaling.

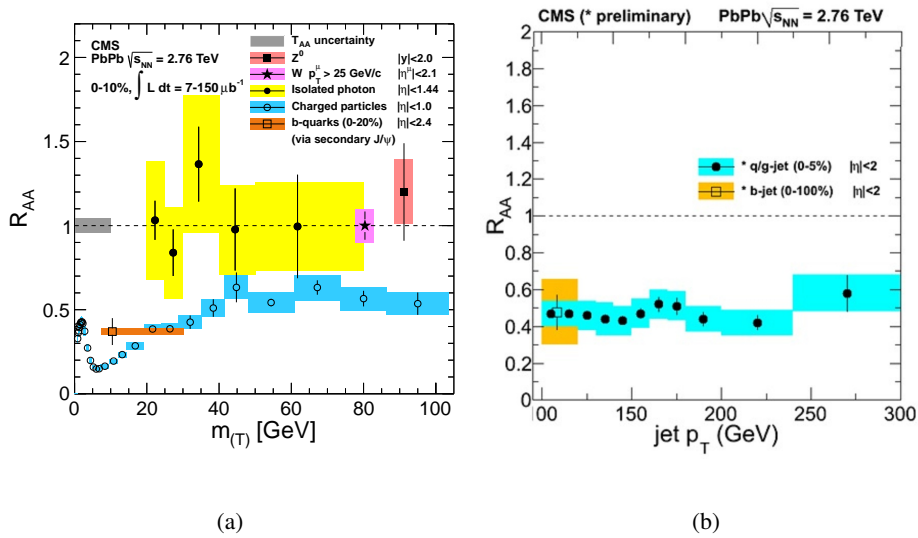


**Figure 3:** a) Collection of CMS nuclear modification factor measurements for a variety of particle species: inclusive charged hadrons, isolated (direct) photons,  $W$ - and  $Z$ -bosons, b-quarks. Centrality selection for each measurement is listed on the figure. b) Jet  $R_{AA}$  for 5% most central PbPb events as function of jet  $p_T$ .

It is evident from the measurements of  $R_{AA}$  for charged hadrons, also presented in the Fig. 3 (a), that the suppression of relative hadron production extends to the edge of kinematic regime covered [13]. In the most central PbPb events the suppression levels off at about 50% above 50 GeV/c, with no pronounced  $p_T$ -dependence up to 100 GeV/c. Similar level of suppression is consistently seen in the jet  $R_{AA}$  shown in Fig. 3 (b) [14] as a function of jet  $p_T$ .

The exact mechanisms for parton energy loss remain under discussion, as various scenarios could accommodate the inclusive data. Differential measurements, such as di-jet energy balance [15], jet shape measurements and comparative analysis of jet fragmentation patterns in PbPb and pp data are essential experimental tools to constrain the model parameters and to gain deeper insights into the nature of QCD interactions in the medium.

Figure 4 shows preliminary CMS results for jet fragmentation functions from run 2011. This measurement of detailed energy distribution among the jet fragments updates the earlier CMS work [16] by extending the measurement to the lower  $p_T$  hadrons (down to 1 GeV/c). For each centrality bin studied (from 50-100% peripheral events to top 10% most central PbPb collisions) the measured fragmentation function is compared to the reference derived from pp data at the same

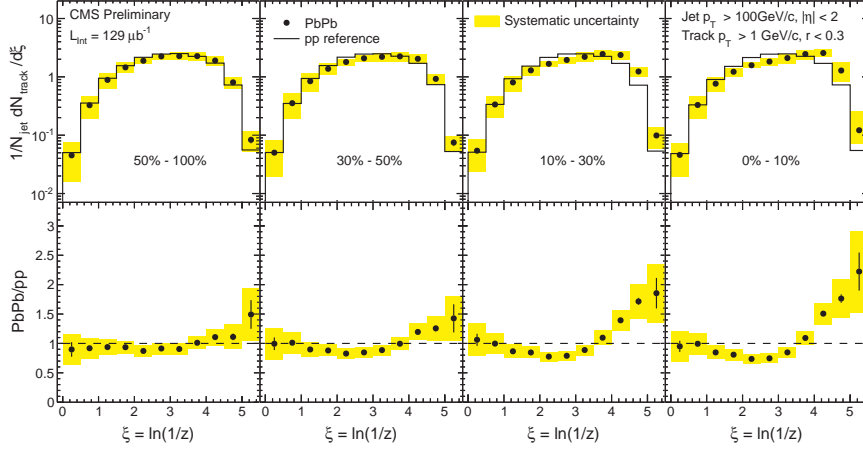


**Figure 4:** Top panel: fragmentation functions for different centrality bins of PbPb collisions at 2.76 TeV are compared with the corresponding reference from pp data at the same energy. The centrality selection ranges from 50-100% peripheral events (leftmost plot) to 0-10% most central collisions (on the right). The jets are selected with  $p_T > 100$  GeV/c. Fragmentation functions are built with all tracks with  $p_T > 1$  GeV/c. Bottom panel: ratio of PbPb and pp fragmentation functions for the corresponding centrality bin from the upper panel. Error bars represent statistical errors, while bands estimate systematic uncertainty in the measurement.

energy. The reference is obtained by smearing (to account for resolution differences) and reweighting (to account for possible differences in the spectral distributions) the measured jet fragmentation function for pp collisions (for details see [17]). In this work the jets are selected to have transverse momentum of at least 100 GeV/c, which ensures nearly perfect jet trigger efficiency. Distributions of jet fragments are plotted as a function of  $\xi = \ln \frac{1}{z}$ ,  $z = \frac{p_{\parallel}^{\text{track}}}{p^{\text{jet}}}$ , where  $p^{\text{jet}}$  is jet momentum and  $p_{\parallel}^{\text{track}}$  is component of the track momentum parallel to the jet axis. To better visualize the differences, the ratio of PbPb to pp fragmentation functions is taken for each centrality bin and shown in the lower panel of Fig. 4. In most peripheral PbPb data the fragmentation functions are found to be very similar between the two systems (with a corresponding ratio of 1). For more central PbPb collisions the jet fragmentation functions become progressively different from the pp reference at intermediate and high  $\xi$  values (e.g. for softer jet fragments between about 1 and 3 GeV/c). The observed excess of charged hadrons in high- $\xi$  region for central events could be taken as an evidence of fragmentation softening due to in-medium interactions.

Redistribution of jet energy towards softer hadrons observed in the fragmentation function measurements, is augmented by studies of the angular distribution of fragments within the jet. The differential jet shape measurements were carried out for the same data selection as in the fragmentation analysis: the reconstructed jets were required to have transverse momentum of at least 100 GeV/c within the jet-cone of radius  $R = 0.3$ . The charged tracks within the jet were measured down to transverse momentum of 1 GeV/c. The jet shapes  $\rho(r)$  are defined as the fraction of jet energy within a differential cone  $dr$  at a given radial distance  $r$  from the jet axis. Preliminary results of differential jet shape measurements from run 2011 are shown in Fig. 5. The upper panel presents centrality evolution of the measurement, starting from 50-100% most peripheral events (on

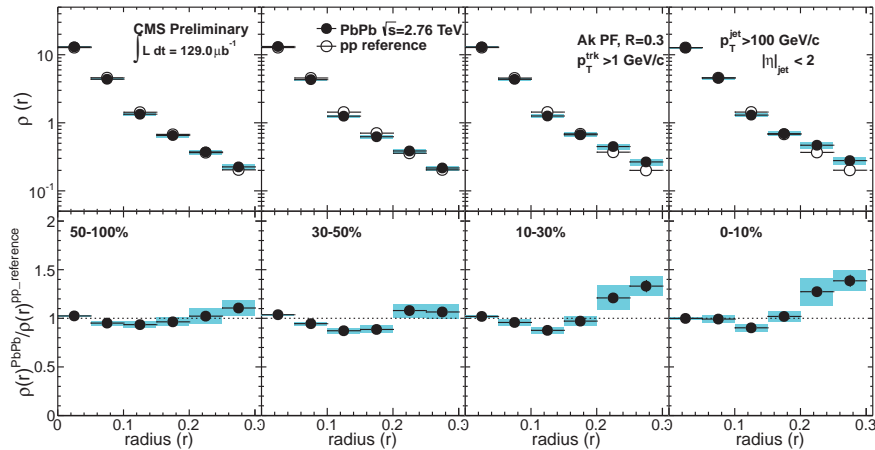


**Figure 5:** Top panel: differential jet shapes for several centrality bins of PbPb collisions at 2.76 TeV are compared with the corresponding reference from pp collisions at the same energy. The centrality selection ranges from 50-100% peripheral events (leftmost plot) to 0-10% most central collisions (on the right). The jets are selected with  $p_T > 100$  GeV/c. Jet shapes are studied with all tracks with  $p_T > 1$  GeV/c inside the jet cone of  $R < 0.3$ . Bottom panel: ratio of PbPb and pp differential jet shapes for each corresponding centrality bin from the upper panel. Error bands show estimate of systematic uncertainty in the measurement.

the left), to the top 10% most central events (on the right). On each plot, a reference distribution, derived from pp data at the same energy, is shown for comparison. Again, lower panel shows the ratio of the differential jet shapes from PbPb and pp data for each of the centrality bins above to help visualize the differences. The peripheral events show no variations between the two systems, with the ratio of differential jet shapes consistent with unity (within errors) across the entire range of radii. The deviation from unity begins to develop at large  $r$  in more central events, becoming most pronounced in the most central bin. The excesses of hadrons at large distance from jet axis found in jets from central PbPb collisions indicates appreciable broadening of jet structure.

## 5. Heavy flavor measurements

The higher integrated luminosity data of run 2011 allowed major advances in the studies of heavy flavor production and in-medium interaction effects for  $c$  and  $b$  quarks. These new data enabled first detailed studies of centrality dependence for quarkonia production. Relative suppression of different quarkonia species is one of the long standing signature predictions of the quark-gluon plasma formation. The suppression, expected to originate from colour screening of the binding potential for quarkonium states from abundant gluons and light quarks, is considered as one of the most direct evidence for the deconfinement. Additionally, studies of quarkonia suppression in heavy ion collisions are expected to aid our understanding of degree of medium thermalization. It is predicted [18, 19] that different quarkonium states will "melt" sequentially, depending on the interplay between their binding energies and the medium temperature. Because of this interplay, the degree of the melting for various quarkonia states is also long proposed as experimental QGP thermometer [20].

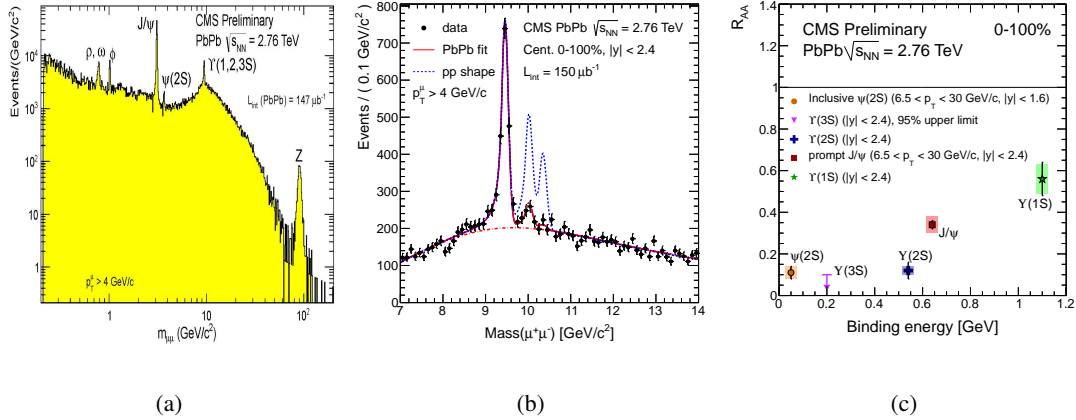


**Figure 6:** a) Invariant-mass spectrum of  $\mu^+\mu^-$  pairs from minimum bias PbPb collisions at 2.76 TeV. b)  $\Upsilon$ ,  $\Upsilon'$  and  $\Upsilon''$  states measurements from minimum bias PbPb data. The solid line shows the form fit to the data used to extract the integrated yields for each state. The dashed line is the result of the form-fit from pp reference data matched to the  $\Upsilon$  yield. c) Nuclear modification factors ( $R_{AA}$ ) for various quarkonia states for minimum bias PbPb collisions.

Figure 6 (a) shows invariant-mass spectrum of  $\mu^+\mu^-$  pairs from minimum bias PbPb collisions at 2.76 TeV. The superb resolution of the CMS muon system, illustrated by the figure, enables clean separation of quarkonia states (with many states clearly visible even before the combinatorial background is subtracted). Panel (b) in the same figure zooms in on the mass range of  $\Upsilon$  family. The data points show di-muon invariant mass distribution with the peaks for  $\Upsilon$ ,  $\Upsilon'$  and  $\Upsilon''$  states from the minimum bias PbPb data [21]. The  $\Upsilon$  and  $\Upsilon'$  peaks are clearly visible, while the  $\Upsilon''$  peak is hard to identify. The solid line shows the form fit to the data used to extract the integrated yields for each state. The reference measurement from pp data at the same energy is also shown in the Fig. 6 (b) as a dashed line. This dashed line is obtained by invariant mass fit to pp data, and then the otherwise fixed shape is scaled to match the  $\Upsilon$  yield from the PbPb collisions. Comparing the PbPb and pp fit lines the nearly complete melting of  $\Upsilon''$  and significant suppression of  $\Upsilon'$  relative to the expected in-vacuum produced abundances is evident. The last panel of Fig. 6 summarizes the available suppression measurements for various quarkonia states from the CMS experiment. The nuclear modification factors are presented to test the sequential melting prediction. Minimum bias PbPb results [22, 23, 24] show the lowest  $R_{AA}$  value (strongest suppression) for  $\psi(2S)$  and  $\Upsilon'$ , and the highest one (least suppressed) for the  $\Upsilon$ , with the  $J/\psi$  measurement falling in between (we note that only an upper limit on the  $\Upsilon''$   $R_{AA}$  is estimated at this point). The  $R_{AA}$  value ordering is consistent with ordering of the binding energies of the quarkonia states [25] and the sequential melting scenario in the QGP medium.

## 6. Summary

In this work a brief review of selected CMS results from PbPb collisions at a center of mass energy of 2.76 TeV from run 2011 is presented. This recent data set, corresponding to an integrated luminosity of  $150 \mu\text{b}^{-1}$ , significantly improves the physics reach for the CMS heavy ion studies.

Additionally, many smaller cross-section measurements have benefited from the CMS High Level Trigger capabilities fully implemented in the run.

Detailed studies of medium properties via angular correlation analyses confirmed the significance of the initial state fluctuations imprinted on the final state particles. Centrality and transverse momentum dependence of higher order Fourier harmonics ( $v_n$ ) provide precise set of measurements to constrain the medium properties, specifically the  $\eta/s$  ratio.

Various measurements presented, update the earlier findings on jet quenching. Nuclear modification factors for colorless probes ( $W$ ,  $Z$  and isolated photons) are found to be consistent with unity within (admittedly) large errors, confirming the relevance of the binary scaling hypotheses for hard probes production. At the same time, strong suppression of charged hadrons is established with significantly improved precision. No appreciable  $p_T$  dependence is found in their  $R_{AA}$  values above 50 GeV/c, of about 0.5 for the most central collisions. This constant  $R_{AA} \approx 0.5$  extends up to 100 GeV/c for reconstructed tracks and up to 300 GeV for jets.

We observe jet modifications in response to the medium in jet shape and fragmentation function measurements. While in peripheral events both jet properties are found to be consistent with the reference derived from pp data at the same energy, broadening of the jet shapes and softening of the jet fragmentation functions gradually set in as the collisions become more central.

The increase in the integrated luminosity recorded made possible new observations in the heavy flavor sector. First detailed centrality dependence studies of nuclear modification factors for quarkonia states have been initiated. The new data have allowed to firmly establish the sequential melting of  $\Upsilon$  states; the hierarchy of suppression was found to be consistent with expectations based on binding energies, and overall suppression is found to increase with collision centrality.

## References

- [1] S. Chatrchyan, *et al.* (CMS Collaboration), *The CMS experiment at the CERN LHC*, JINST **3** (2008) S08004.
- [2] S. Chatrchyan, *et al.* (CMS Collaboration), *Observation and studies of jet quenching in PbPb collisions at nucleon nucleon center-of-mass energy = 2.76 TeV*, Phys. Rev. C **84** (2011) 024906.
- [3] S. Chatrchyan, *et al.* (CMS Collaboration), *Measurement of the elliptic anisotropy of charged particles produced in PbPb collisions at  $\sqrt{s_{NN}}=2.76$  TeV*, Phys. Rev. C **87** (2013) 014902.
- [4] CMS Collaboration, CMS Public Heavy Ion Results, <https://twiki.cern.ch/twiki/bin/view/CMSPublic/PhysicsResultsHIN>.
- [5] S. A. Voloshin, A. M. Poskanzer and R. Snellings, *Collective phenomena in non-central nuclear collisions*, Landolt-Börnstein Database “Relativistic Heavy Ion Physics” Vol. **23** (2010).
- [6] S. Chatrchyan, *et al.* (CMS Collaboration), *Centrality dependence of dihadron correlations and azimuthal anisotropy harmonics in PbPb collisions at  $\sqrt{s_{NN}}=2.76$  TeV*, Eur.Phys.J. C **72** (2012) 2012.
- [7] B. Schenke, S. Jeon, C. Gale, *Higher flow harmonics from (3+1)D event-by-event viscous hydrodynamics*, arXiv:1109.6289.
- [8] S. Chatrchyan, *et al.* (CMS Collaboration), *Azimuthal anisotropy of charged particles at high transverse momenta in PbPb collisions at  $\sqrt{s_{NN}} = 2.76$  TeV*, Phys. Rev. Lett. **109** (2012) 022301.

- [9] B. Betz and M. Gyulassy, *Examining a reduced jet-medium coupling in Pb+Pb collisions at the Large Hadron Collider*, Phys. Rev. C **86** (2012) 024903.
- [10] S. Chatrchyan, *et al.* (CMS Collaboration), *Measurement of isolated photon production in pp and PbPb collisions at 2.76 TeV*, Phys. Lett. B **710-2** (2012) 256.
- [11] S. Chatrchyan, *et al.* (CMS Collaboration), *Study of Z boson production with  $150 \mu\text{b}^{-1}$  integrated PbPb luminosity at  $\sqrt{s_{NN}}=2.76 \text{ TeV}$* , CMS PAS HIN-12-008, <http://cds.cern.ch/record/1472723>.
- [12] S. Chatrchyan, *et al.* (CMS Collaboration), *Study of W boson production in PbPb and pp collisions at  $\sqrt{s_{NN}}=2.76 \text{ TeV}$*  Phys. Lett. B **715** (2012) 66.
- [13] S. Chatrchyan, *et al.* (CMS Collaboration), *Study of high- $p_T$  charged particle suppression in PbPb compared to pp collisions at  $\sqrt{s_{NN}}=2.76 \text{ TeV}$* , Eur. Phys. J. C **72** (2012) 1945.
- [14] S. Chatrchyan, *et al.* (CMS Collaboration), *Nuclear modification factor of high transverse momentum jets in PbPb collisions at  $\sqrt{s_{NN}}=2.76 \text{ TeV}$* , CMS-PAS HIN-12-004, <http://cds.cern.ch/record/1472722>.
- [15] S. Chatrchyan, *et al.* (CMS Collaboration), *Observation and studies of jet quenching in PbPb collisions at  $\sqrt{s_{NN}}=2.76 \text{ TeV}$* , Phys. Rev. C **84** (2011) 024906.
- [16] S. Chatrchyan, *et al.* (CMS Collaboration), *Measurement of jet fragmentation into charged particles in pp and PbPb collisions at  $\sqrt{s_{NN}}=2.76 \text{ TeV}$* , JHEP **10** (2012) 087.
- [17] S. Chatrchyan, *et al.* (CMS Collaboration), *Jet fragmentation functions in PbPb and pp collisions at 2.76 TeV with CMS*, CMS PAS HIN-12-013, <http://cds.cern.ch/record/1472734>.
- [18] H. Satz, *Quarkonium Binding and Dissociation: The Spectral Analysis of the QGP*, Nucl. Phys. A **783** (2007) 249.
- [19] H. Satz, *Colour Deconfinement and Quarkonium Binding*, J. Phys. G **32** (2006) R25.
- [20] A. Mocsy, *Potential Models for Quarkonia*, Eur.Phys.J. C **61** (2009) 705.
- [21] S. Chatrchyan, *et al.* (CMS Collaboration), *Observation of Sequential  $\Upsilon$  Suppression in PbPb Collisions* Phys. Rev. Lett. **109** (2012) 222301.
- [22] S. Chatrchyan, *et al.* (CMS Collaboration), *Suppression of non-prompt  $J/\psi$ , prompt  $J/\psi$ , and  $\Upsilon(1S)$  in PbPb collisions at  $\sqrt{s_{NN}}=2.76 \text{ TeV}$* , JHEP **05** (2012) 063.
- [23] S. Chatrchyan, *et al.* (CMS Collaboration), *Measurement of the  $\psi(2S)$  meson in PbPb collisions at  $\sqrt{s_{NN}}=2.76 \text{ TeV}$* , CMS PAS HIN-12-007, <http://cds.cern.ch/record/1455477>.
- [24] S. Chatrchyan, *et al.* (CMS Collaboration),  *$J/\psi$  results from CMS in PbPb collisions, with  $150\mu\text{b}^{-1}$  data*, CMS PAS HIN-12-014, <http://cds.cern.ch/record/1472735>.
- [25] L. Kluberg and H. Satz, *Color Deconfinement and Charmonium Production in Nuclear Collisions*, arXiv:0901.3831.